



**University of
Zurich**^{UZH}

**Zurich Open Repository and
Archive**

University of Zurich
University Library
Strickhofstrasse 39
CH-8057 Zurich
www.zora.uzh.ch

Year: 2017

Role of the OATP Transporter Family and a Benzbromarone-Sensitive Efflux Transporter in the Hepatocellular Disposition of Vincristine

Nicolaï, Johan ; Thevelin, Louise ; Bing, Qi ; Stieger, Bruno ; Chanteux, Hugues ; Augustijns, Patrick ;
Annaert, Pieter

DOI: <https://doi.org/10.1007/s11095-017-2241-0>

Posted at the Zurich Open Repository and Archive, University of Zurich

ZORA URL: <https://doi.org/10.5167/uzh-141559>

Journal Article

Accepted Version

Originally published at:

Nicolaï, Johan; Thevelin, Louise; Bing, Qi; Stieger, Bruno; Chanteux, Hugues; Augustijns, Patrick;
Annaert, Pieter (2017). Role of the OATP Transporter Family and a Benzbromarone-Sensitive Efflux
Transporter in the Hepatocellular Disposition of Vincristine. *Pharmaceutical Research*, 34(11):2336-
2348.

DOI: <https://doi.org/10.1007/s11095-017-2241-0>

Title page

Title: Role of the OATP transporter family and a benzbromarone-sensitive efflux transporter in the hepatocellular disposition of vincristine.

Authors: Johan Nicolai^{1,3}, Louise Thevelin¹, Qi Bing¹, Bruno Stieger², Hugues Chanteux³, Patrick Augustijns¹, Pieter Annaert¹

Affiliations:

¹Drug Delivery and Disposition, KU Leuven Department of Pharmaceutical and Pharmacological Sciences, O&N2, Herestraat 49 - box 921, 3000 Leuven, Belgium

² Department of Clinical Pharmacology and Toxicology, University Hospital, Zürich, Switzerland

³ UCB Pharma S.A., Non-Clinical Development, B-1420 Braine l'Alleud, Belgium

Running head: OATP-mediated hepatocellular disposition of vincristine

Corresponding author:

Pieter P. Annaert

Drug Delivery and Disposition

KU Leuven Department of Pharmaceutical and Pharmacological Sciences

O&N2, Herestraat 49 - box 921

B-3000 Leuven

Belgium

E-mail address: pieter.annaert@kuleuven.be

Tel: +32 16 3 30303 or +32 16 3 30300

Fax: +32 16 3 30305

Abstract

Purpose: Vincristine is known to interfere with OATP-mediated uptake of other compounds, hinting that vincristine itself could be a substrate of OATP transporters. The present study therefore aimed to investigate the role of OATP transporters in the hepatocellular disposition of vincristine.

Methods: Vincristine uptake was studied in suspended rat and human hepatocytes as well as OATP-transfected Chinese hamster ovary (CHO) cells in the absence and presence of OATP transporter inhibitors. Membrane vesicles containing MDR1 or MRP1/2/3 were used to directly assess the role of these efflux transporters in vincristine disposition.

Results: Uptake in suspended rat hepatocytes was temperature-dependent and could be inhibited by a range of OATP inhibitors. Furthermore, the MRP-inhibitor benzbromarone, but none of the tested MDR1 inhibitors, reduced vincristine efflux in rat and human suspended hepatocytes. OATP1B1-, OATP1B3- and OATP2B1- transfected CHO cells showed significantly increased vincristine uptake as compared to wild-type cells. Moreover, uptake in OATP-transfected CHO cells was reduced by OATP inhibitors. However, uptake studies in suspended human hepatocytes showed that only 10% of the total vincristine uptake process could be attributed to OATP-mediated transport. Studies with transporter-expressing membrane vesicles confirmed vincristine as an MDR1 substrate, while MRP1/2/3-mediated transport of vincristine could not be observed with this model system.

Conclusions: Our findings show the involvement of OATP transporters in the disposition of vincristine in rat and human hepatocytes. However, in both species, hepatic uptake is overshadowed by a benzbromarone-sensitive efflux mechanism, possibly MRP3.

Keywords

Vincristine; OATP; MRP; Benzbromarone; Hepatocytes

Abbreviations

ABC	ATP-binding cassette
CHO	Chinese hamster ovary
Cl	Clearance
MRP	Multidrug resistance-associated protein
OATP	Organic anion transporting polypeptide
RAF	Relative activity factor
SHH	Suspended human hepatocytes
SLC	Solute carrier
SRH	Suspended rat hepatocytes

Introduction

Since its identification in the early 60's in extracts originating from the *Catharanthus roseus* flower (Madagascar periwinkle), vincristine has been a key chemotherapeutic drug for the treatment of both adult and pediatric cancer patients (1). Vincristine is a cornerstone during the induction, intensification and consolidation phases in the treatment of acute lymphoblastic leukemia (2, 3). Moreover, it is indicated for Hodgkin lymphoma, non-Hodgkin lymphoma, neuroblastoma, rhabdomyosarcoma and Wilms tumor (4). Vincristine cytotoxicity arises from microtubule binding, which disrupts the mitotic spindle during cell division, causing cell cycle arrest and inducing apoptosis (5). This mechanism of action requires an adequate intracellular exposure. However, intracellular vincristine concentrations are hard to predict due to drug resistance factors such as P-gp/ABCB1/MDR1 and members of the MRP/ABCC family (6). Additionally, large inter-individual variability in vincristine pharmacokinetics (>30%) as well as a high risk for dose-dependent vincristine-induced neuropathy hamper selection of a suitable dose (5). A thorough understanding of vincristine disposition could help identify key mechanisms underlying vincristine pharmacokinetics, pharmacodynamics and toxicity. Incorporation of this information into physiologically-based pharmacokinetic (PBPK) and population-PK models, could aid in improving patient-specific dosing guidelines. Vincristine pharmacokinetics is defined by a large volume of distribution (160 L/m²) and a relatively long terminal elimination half-life (8.2 h), determined primarily by hepatobiliary elimination and to a lesser extent by renal elimination (7). Initial studies with radiolabeled vincristine showed a 40-fold higher vincristine concentration in the bile as compared to plasma (8). These studies also indicated that after 72 hours, 8 to 15% of the administered dose can be found in urine and about 70% can be recovered from feces, of which 50 to 60% unchanged. Even though only 50% of the administered dose is metabolized, CYP3A5 expression has been inversely correlated with the risk of developing vincristine-induced

neuropathy (9). Additionally, concomitant treatment of vincristine with CYP3A4/5 inhibitors, like the azole-type antifungals, increases the risk for vincristine-induced neuropathy (10). Notably, CYP3A5-mediated vincristine clearance is 9 to 14-fold higher as compared to CYP3A4-mediated clearance (11). Consequently, CYP3A4 only contributes significantly to vincristine metabolism in CYP3A5 non-expressers (11-13). Apart from CYP3A4/5, vincristine is also a substrate for several ABC-transporters i.e.: P-gp/ABCB1/MDR1 (14), MRP1/ABCC1 (15) and MRP2/ABCC2 (16). Furthermore, presence of MRP3/ABCC3 (17), MRP7/ABCC10 (18), ABCB6 (19) and RALBP1 (20) have been shown to increase resistance to vincristine toxicity. Resistance to chemotherapeutics due to (enhanced) expression and action of efflux transporters received a lot of attention in the past. More recently, the importance of SLC-transporters for the uptake of chemotherapeutics into tumor cells and for pharmacokinetics of chemotherapeutics has also gained a lot of interest (21-23). Overexpression of SLC-transporters (e.g. OATP1B3) in certain cancer types could sensitize tumor cells for chemotherapeutics which are substrates of these uptake transporters. Yet, apart from the chemo-sensitizing effect of the kidney-specific OCT3/SLC22A3 transporter in kidney carcinoma cell lines (24), no uptake transporter has been linked to vincristine disposition. Nevertheless, some reports show that vinca-alkaloids can accumulate strongly in HL-60 cells and interact with carrier-mediated processes in rat/human hepatocytes and murine leukemia cells (25-28). Additionally, vincristine has been shown to interfere with OATP1B1- and OATP1B3-mediated substrate transport (29-31). Therefore, the aim of the present work was to investigate whether hepatic isoforms of the OATP transporter family play a role in the hepatocellular disposition of vincristine in rat and human hepatocytes.

Materials and Methods

Materials

Vincristine-sulfate was acquired from LC chemicals (Woburn, Massachusetts); vinblastine (1 mg/ml) as well as methotrexate (2.5 mg/ml) were obtained from TEVA Pharma Belgium (Wilrijk, Belgium). Atazanavir-sulfate was obtained through the NIH Aids Reagent Program. Benzbromarone, bromosulphophthalein, 5(6)-Carboxy-2',7'-dichlorofluorescein (CDCF), digoxine, glibenclamide, losartan, paclitaxel, paraffin oil, L-proline, rifampycine, rifamycine SV and silicon oil (AP150) were purchased from Sigma-Aldrich (Schnelldorf, Germany). Dulbecco's modified eagle medium (DMEM; 1g/L glucose, 25 mM HEPES), fetal bovine serum (heat-inactivated) (FBS), L-glutamine (200 mM), Hanks' Balanced Salt Solution (HBSS), penicillin-streptomycin mixture (10,000 IU potassium penicillin and 10,000 IU streptomycin sulfate per ml in 0.85 % saline), phosphate buffered saline (PBS), trypsin- EDTA mixture (170 U/ml and 200 mg/L, respectively) and Trypan blue stain (0.4 %) were obtained from Westburg (Leusden, The Netherlands). Dimethylsulfoxide (DMSO), methanol (MeOH) and Na-pyruvate were purchased from Acros Organics (Geel, Belgium). CaCl_2 and NaHCO_3 were obtained from Chem-lab NV (Zedelgem, Belgium) and NaCl from Fisher Chemical (Landsmeer, The Netherlands). Geneticine-sulfate was purchased from Life Technologies (Paisley, UK) and HEPES (4-(2-hydroxyethyl)-1-piperazineethanesulfonic acid) from MP Biochemical (Illkrich, France). $\text{MgCl}_2 \cdot 7\text{H}_2\text{O}$ was obtained from Analar-Normapur (VWR) (Leicestershire, England) and KCl from AppliChem GmbH (Darmstadt, Germany). Cyclosporine A was purchased from Sequoia Research Products LTD (Pangbourne, UK). MK-571 was obtained from Merck chemicals (Overijse, Belgium) and docetaxel from Avantis Pharma (Diegem, Belgium). Quinidine-sulfate was purchased from Unibios lab (Mumbai, India) and Formic acid (LC-MS grade) from

Biosolve-chemicals (Valkenswaard, The Netherlands). Control, MRP1, MRP2, MRP3 and MDR1 inside-out membrane vesicles were purchased from ThermoFisher Scientific (Waltham, MA USA). Estradiol 17-(β -D-Glucuronide) was purchased from Sanbio (Uden, The Netherlands).

Animals

Male Wistar rats were purchased from Janvier (Le Genest Saint Isle, France) and housed according to Belgian and European laws, guidelines and policies for animal experiments, animal housing, and animal care in the Central Animal Facility of the KU Leuven. All experiments involving lab animals were approved by The Institutional Ethical Committee for Animal Experimentation (license number: LA 1210261).

Vincristine uptake in suspended rat hepatocytes

Suspended hepatocytes from Wistar rats (190-200g) were isolated according to the two-step collagenase perfusion method, cryopreserved and thawed as described previously. (32). Freshly-isolated hepatocytes were suspended in Krebs-Henseleit buffer (KHB) (118 mM NaCl; 5.17 mM KCl; 1.2 mM CaCl_2 ; 1.2 mM MgCl_2 ; 23.8 mM NaHCO_3 ; 12.5 mM HEPES; 11.1 mM Glucose; 5 mM Na-pyruvate; pH 7.4) sparged with carbogen (95%:5% O_2 : CO_2) and kept at 4°C until the start of the experiment. Viability and cell density were evaluated using the Trypan blue (0.04%) exclusion method and counting on a hemocytometer. Viability of freshly-isolated hepatocytes ranged between 90 and 92% and viability of cryopreserved hepatocytes was 81%. Cells were diluted to a two-fold concentrated cell density (2 million cells/ml) before the start of experiments. Incubations were initiated by adding 175 μL of four-fold concentrated inhibitor solution to 350 μL of the two-fold concentrated cell suspension in a glass test tube and pre-incubating for 10 min

at 37°C. Following the pre-incubation, 175 µl of four-fold concentrated (2 µM) vincristine solution in KHB was added. Uptake of vincristine in suspended rat hepatocytes was linear as a function of time up to 3 min (data not shown). After 3 min, three 200 µL aliquots of the incubate were layered on top of 700 µL of oil (82:18 silicon oil AP150:paraffin oil; density 1.051 g/ml) which itself had been layered on top of 300 µL of 8% NaCl solution in 1.5 ml centrifuge tubes. Tubes were centrifuged immediately for 3 min at 16,162 g. Following centrifugation, centrifuge tubes were placed in ethanol cooled with dry ice (-80°C), where they were kept until the end of the experiment. After finishing the experiments, the bottom of the tubes were cut (\pm 80 µL) and collected in glass test tubes. Pellets were lysed by shaking them for 30 min after adding 300 µL of 70:30 MeOH:H₂O containing 2.5 nM of the internal standard (vinblastine). After the pellets were completely disrupted, lysates were collected in 1.5 ml centrifuge tubes and stored at -80°C until the day of analysis.

Culturing of Chinese hamster ovary cells

Wild-type, OATP1B1-, OATP1B3-, and OATP2B1-transfected CHO cells were cultured at passage numbers 75–77, 67-69, 67-69 and 27-29, respectively. The CHO cells were grown in a humidified incubator (37°C, 5% CO₂) in T-75 cm² culture flasks (Greiner Bio-One, Wemmel, Belgium) containing 15 ml of culture medium. Culture medium consisted of DMEM (1g/L glucose; 25 mM HEPES) supplemented with 10% FBS, 50 µg/ml L-proline, 100 U/ml penicillin, 100 µg/ml streptomycin, 2 mM L-glutamine and 110 µg/ml sodium pyruvate. Medium of OATP-transfected cells was supplemented with 500 µg/ml of geneticin. When cells were 90-100% confluent, culture medium was removed and cells were washed two times with 1.5 ml of trypsin-EDTA mixture, prewarmed at 37°C. This was followed by adding 2 ml of the trypsin-EDTA mixture to the cells and keeping them in a humidified incubator (37°C, 5% CO₂) for 4

min. After cells were detached, trypsinization was stopped by adding 8 ml of culture medium. Cells were counted on a hemocytometer and subcultured at a ratio depending on the acquired cell count. In preparation of uptake experiments, cells were seeded at a density of 20,000 – 25,000 per well in Advanced TC™ 24-well plates (Greiner Bio-One, Wemmel, Belgium). Medium was replaced every other day and experiments were performed after CHO-cells reached 90-100% confluence on day four after seeding. One day before the experiments, CHO-cells were treated with 5 mM of sodium butyrate in culture medium to induce gene expression.

Vincristine uptake in transfected Chinese hamster ovary cells

On the day of experiments, cell morphology and confluence were visually checked. Cells were washed twice with 0.5 ml/well of warm (37°C) HBSS (10 mM HEPES, pH 7.4) and pre-incubated for 10 min with 250 µL of warm (37°C) KHB with or without a two-fold concentrated uptake transporter inhibitor solution (20 µM). Following pre-incubation, 250 µL of warm (37°C) two-fold concentrated vincristine solution (20 µM; KHB) was added. Linearity studies were performed to ensure linear uptake of vincristine for at least 3 min (data not shown). After 3 min, the incubate was aspirated and cells were washed four times with ice-cold (4°C) HBSS (10 mM HEPES, pH 7.4). Subsequently, cells were lysed for 30 min with 300 µl of 70:30 MeOH:H₂O containing 2.5 nM of vinblastine as internal standard. Lysates were transferred to 1.5 ml centrifuge tubes and stored at -80°C until the day of analysis. A control plate was included which was incubated with a positive control (sodium fluorescein) to verify OATP activity (data not shown). Cells in the control plate were lysed with 300 µL of 0.5% Triton-X in PBS. These lysates were used to measure the protein content using a BCA Protein Assay kit (Pierce Chemical, Rockford, IL, USA), enabling normalization of uptake rates for protein content. Uptake of vincristine in wild-type (Wt)-cells was subtracted from uptake of vincristine in transfected CHO-

cells to calculate the net uptake, which equals the transporter-mediated component of vincristine in the OATP-transfected CHO-cells.

Vincristine uptake in suspended human hepatocytes

Cryopreserved human hepatocytes were acquired in collaboration with BioreclamationIVT[®] (Brussels, Belgium). Human hepatocytes donor information per batch is shown in Table 1. Cells were stored in liquid nitrogen (-196°C) until the day of experiments. On the day of the experiment, cells were thawed by gently shaking the vial in a water bath (37°C). When frozen liquid was no longer present, the content of the vial was transferred completely into a 50 ml Falcon[®] tube containing warm (37°C) InVitroGRO[™] HT thawing medium (BioreclamationIVT[®], Brussels, Belgium). The hepatocyte suspension was centrifuged for 5 min (50 g) at 21°C, supernatant was aspirated and the pellet gently resuspended in 1 ml of warm (37°C) KHB. Viability and cell density were evaluated using the Trypan blue (0.04%) exclusion method and counting on a hemocytometer. Viability of human hepatocytes ranged between 80 and 92%. Prior to the experiment, cells were diluted to a two-fold concentrated cell density (2 million cells/ml). Pre-incubation and uptake experiments were performed similar to uptake experiments performed with SRH. However, contrary to the oil-spin method applied with SRH, direct centrifugation was applied for SHH. This was done because benzbromarone decreased the passage of SHH through the oil-layer in a concentration dependent manner (data not shown). After 1 min incubations, 200 µL aliquots were transferred to 1.5 ml centrifuge tubes which were centrifuged for 30 sec at 16,162 g. Next, supernatants were aspirated and pellets were washed with ice cold (4°C) PBS, followed by a repetition of the centrifugation step. Following centrifugation, the PBS was aspirated and 300 µL of ice cold (4°C) 8% NaCl was added on top of the pellets. After a final centrifugation, centrifuge tubes were placed in ethanol cooled with dry

ice (-80°C), where they were kept until the end of the incubations. After finishing the experiments, the bottom of the tubes were cut (\pm 80 μ L) and collected in glass test tubes. Pellets were lysed by shaking them for 30 min after adding 300 μ L of 70:30 MeOH:H₂O containing 2.5 nM of the internal standard (vinblastine). After the pellets were completely disrupted, lysates were collected in 1.5 ml centrifuge tubes and stored at -80°C until the day of analysis.

Vincristine uptake in inside-out membrane vesicles

Just before the experiment, vesicles (control, MRP1, MRP2, MRP3, MDR1) were thawed by gently shaking in a water bath (37°C) and were kept on ice (4°C) until dilution. Prior to experiments, vesicles (5 mg/mL) were diluted in vesicle uptake buffer (50 mM MOPS-TRIS; 70 mM KCl; 7.5 mM MgCl₂; pH 7) and dispensed (29 μ L) in 2 mL Eppendorf® tubes. Diluted vesicles were pre-incubated for 5 minutes in a shaking water bath (37°C; 70 rpm). Incubations were initiated by addition of 21 μ L of reaction mixture in vesicle uptake buffer to obtain following final concentrations: 4 mM ATP or AMP; 5 mM reduced glutathione; 0.1% v/v DMSO or 100 μ M benzbromarone; 200 nM of vincristine or 10 μ M of 5(6)-Carboxy-2',7'-dichlorofluorescein (CDCF) or estradiol 17- β -D-glucuronide (E17BDG). Positive control substrates (CDCF, E17BDG) were incubated for 3 minutes and uptake of vincristine was assessed for 5 minutes. Uptake was stopped by addition of 200 μ L ice-cold (4°C) stop buffer (40 mM MOPS-TRIS; 70 mM KCl; pH 7) and subsequent vortexing. Samples were stored at 4°C until the end of the experiment. 200 μ L of the stopped incubate was filtered using a vacuum manifold (Merck-Millipore®) and 96-well 1 μ m pore-size glass-fiber filter plates (MSFBN6B10; Merck-Millipore®) presoaked with 200 μ L ice-cold (4°C) stop buffer. Wells containing vincristine were washed 5 times with 200 μ L of ice-cold stop buffer containing 1% w/v BSA, subsequently 5 times with 200 μ L of ice-cold stop-buffer containing 0.05% v/v Tween-20 and

finally 5 times with 200 μ L of ice-cold stop-buffer (14). Wells of all other substrates were washed 5 times with 200 μ L of ice-cold stop buffer. Control wells were included to assess the extent of substrate binding to the filter plate, the blank and the start-solution. Vincristine samples were solubilized using 50 μ L of 70:30 MeOH:H₂O containing 10 nM of the internal standard (vinblastine). E17BDG samples were solubilized using 50 μ L of 70:30 MeOH:H₂O. CDCF samples were solubilized using 50 μ L of 10% w/v SDS. After addition of the correct solubilizing agent, filter plates were placed on top of a 96-well receiver plate and centrifuged for 1 minute at 850 g (21°C). Following centrifugation, the solubilizing and centrifugation step were repeated once more. For compounds analyzed by LC-MSMS, vincristine and E17BDG, 80 μ L of filtrate was transferred to deep-well 96-well plates and evaporated under a gentle stream of N₂ (45°C). Samples were dissolved using 50:50 ACN:H₂O, centrifuged and injected onto the LC-MSMS system. 80 μ L of samples containing CDCF were diluted with 100 μ L of NaOH (0.1 M) and analyzed using fluorescence spectroscopy (Ex : 485 nm, Em : 535 nm; Spectramax[®] M2).

Bioanalysis

On the day of analysis, samples were thawed, vortexed and centrifuged (20,816 g) for 10 min at 4°C. The obtained supernatants were transferred into micro-inserts for LC-MS/MS analysis and injected directly into the LC-MS/MS system. The Thermo Scientific (San Jose, USA) LC-MS/MS system comprised an Accela[®] autosampler, an Accela[®] pump and TSQ Quantum Access[®] triple quadrupole mass spectrometer equipped with an electrospray ionization (ESI) source. A kinetex[®] XB – C18 column (50 mm x 2.1 mm, 2.6 μ m), protected by a SecurityGuard ULTRA precolumn (Phenomenex, The Netherlands), was used for chromatographic separation. The mobile phase consisted of 0.2% v/v formic acid in ELGA[®] water (A), methanol (B) and ELGA[®] water (C). Gradient elution was performed at a constant flow rate (400 μ L/min) as

follows: the mobile phase from the start until 1 min of analysis consisted of 37.5% A, 10% B and 52.5% C, respectively. The percentage of A was kept constant, while B increased linearly up to 62.5% during 2 min, followed by an immediate decrease (0.1 min) to 10% B and a re-equilibration of the system for 1.4 min before the next injection. The total run time was 4.5 min and the injection volume amounted to 10 μ L (partial loop mode) for SRH/CHO samples while it amounted to 25 μ L (full loop mode) for SHH samples. The column oven and sample tray temperatures were set at 30°C and 15°C, respectively. The MS was operated in positive ion mode at a spray voltage of 3,500 V. Argon was used as collision gas at a pressure of 1.5 mTorr. The MS was operated in 3-channel selected reaction monitoring (SRM) mode with a scan time of 75 msec. Transitions monitored were 413.2 \rightarrow 353.1 m/z and 413.2 \rightarrow 383.2 m/z for vincristine (MH^{2+}) and 406.2 \rightarrow 272.6 m/z and 406.2 \rightarrow 376.2 m/z for vinblastine (MH^{2+}) with retention times of 3.02 and 3.14 min for vincristine and vinblastine, respectively. Other ionization parameter settings were: capillary temperature (275°C), vaporizing temperature (300°C), sheet gas pressure (30 arbitrary units), auxiliary gas pressure (25 arbitrary units) and ion sweep gas pressure (0 arbitrary units). Collision energies were 23 and 18 arbitrary units for vincristine and 24 and 17 arbitrary units for vinblastine, respectively. Quality control concentrations were 0.2 μ M, 0.02 μ M and 0.002 μ M for SRH/CHO samples, and 0.1 μ M, 0.01 μ M and 0.001 μ M for SHH samples. Intra- and interday precision of quality control samples were below 10% for the high and middle concentrations and < 15% for the low concentration. The calibration curves were linear over 12 points ranging from 500 to 0.25 nM and from 250 to 0.13 nM for SRH/CHO and SHH samples, respectively.

Data-analysis

ANOVA (α level of 0.05; Dunnett's post hoc test) was applied to compare control conditions to experiments including inhibitors, using Graphpad Prism[®] version 5.00 for windows (GraphPad Software, Inc., California, USA). The Shapiro-Wilk test for normality was applied to test the distribution of SHH data for normality. Subsequently, a grouped two-way Student's t-test was applied (α level of 0.05) to the overall averages to compare the populations with and without inhibitor.

Uptake data from CHO-cell experiments were used to estimate the OATP-mediated uptake clearance of vincristine in SHH as reported by De Bruyn and coworkers (Equation 1) (33).

$$Cl_{OATP1B1/3,SHH} = Cl_{OATP1B1/3,CHO} \times RAF_{OATP1B1/3}$$

(Equation 1)

$Cl_{OATP1B1/3,SHH}$ is the uptake clearance of vincristine by either OATP1B1 or OATP1B3 predicted for SHH. $Cl_{OATP1B1/3,CHO}$ is the uptake clearance of vincristine in either OATP1B1- or OATP1B3-transfected CHO cells and $RAF_{OATP1B1/3}$ is the relative activity factor determined for OATP1B1 or OATP1B3 transfected CHO cells with estrone-3-sulfate and CGamF, respectively (Table 2). RAF-factors determined by De Bruyn and coworkers were determined on the same OATP-transfected CHO cells as applied in the present study and a pool of human hepatocytes (Table 1) (33). Therefore, we deemed it was justifiable to use the same RAF-factors as determined by De Bruyn and coworkers to recalculate the uptake data acquired in CHO cells.

Passive uptake clearance of vincristine in SHH cells ($Cl_{passive,SHH}$) was estimated from vincristine uptake clearance in wild-type CHO cells ($Cl_{wt,CHO}$). After dividing the surface area of CHO cells

by the surface area of SHH, a factor of 0.51 was obtained (33). This factor was applied according to Equation 2 to correct the $Cl_{wt,CHO}$ for the difference in surface area across which passive permeation can occur. Thus, $Cl_{passive,SHH}$ was calculated:

$$Cl_{passive,SHH} = \frac{Cl_{wt,CHO}}{0.51}$$

(Equation 2)

Results

Vincristine uptake in suspended rat hepatocytes

Uptake of vincristine in SRH was found to be temperature-dependent: uptake at 4°C [2.2 ± 0.5 pmol/(min x million cells)] was significantly lower than uptake at 37°C [5.58 ± 0.5 pmol/(min x million cells)] (Figure 1). Additionally, uptake of vincristine in SRH could be inhibited with known inhibitors of OATP-mediated transport (10 μ M) as shown in Figure 1 (atazanavir, bromosulfophthalein, cyclosporine A, docetaxel, glibenclamide, losartan, MK571, methotrexate, paclitaxel, rifampicin, rifamycin SV). However, no statistically significantly different uptake was observed when vincristine was incubated in the presence of digoxin or quinidine. Increasing concentrations of known MRP inhibitors MK571 and benzbromarone significantly increased the intracellular accumulation of vincristine in SRH (Figures 2A and 2B). However, at low concentrations (10 μ M) MK571 also inhibited vincristine uptake.

Vincristine uptake in OATP1B1/1B3/2B1-transfected Chinese hamster ovary cells

The uptake of vincristine was investigated in CHO cells transfected with human OATP1B1, 1B3 and 2B1 and compared to uptake in wild-type CHO cells. Under these conditions, uptake of vincristine was significantly higher in all of the OATP-transfected CHO cells as compared to the uptake in wild-type CHO cells (Figures 3A). Interestingly, uptake in OATP1B3-transfected cells [77.7 ± 6.4 pmol/(min x mg protein)] was noticeably higher than the uptake in OATP1B1- [39.6 ± 5.7 pmol/(min x mg protein)] and 2B1-transfected cells [39.3 ± 4.6 pmol/(min x mg protein)]. Additionally, uptake of vincristine could be significantly inhibited with known inhibitors of OATP-mediated transport (10 μ M) as shown in Figure 3B-D (atazanavir, docetaxel, digoxin, losartan, methotrexate, paclitaxel, rifamycin SV, benzbromarone). Vincristine uptake could not

be saturated in any of these cell lines when incubated at concentrations up to 300 μ M (data not shown). In view of clinical relevance, higher concentrations of vincristine were not evaluated.

Vincristine uptake in suspended human hepatocytes

Effect of temperature, rifamycin SV and benzbromarone on the uptake of vincristine in suspended human hepatocytes was assessed (Figures 4A-C). In all batches of human hepatocytes, a significant decrease of vincristine uptake was observed at 4°C when compared to experiments performed at 37°C (Figure 4A). However, the effect of 10 μ M rifamycin SV on vincristine uptake in SHH was only statistically significant in one batch of human hepatocytes (HRU; $p = 0.0057$), in which it decreased by 52.5%. In all other batches, vincristine uptake decreased by approximately 10% in the presence of 10 μ M rifamycin SV, but these changes were not statistically significant (Figure 4B). Also, increasing the rifamycin SV concentration to 100 μ M did not significantly alter vincristine uptake in SHH (data not shown). Still, in the presence of 100 μ M benzbromarone, vincristine uptake increased to $407 \pm 105\%$ in all batches of SHH as compared to the control condition ($p < 0.0001$), suggesting an involvement of an MRP-mediated efflux process.

Vincristine uptake data from OATP-transfected CHO cells were converted for comparison with uptake data obtained in SHH, by using previously reported RAF factors (Table 3) (33). A good match was observed between passive uptake clearance estimated from uptake in wild-type CHO cells [$4.1 \pm 0.5 \mu\text{l}/(\text{min} \times \text{million cells})$] and passive uptake clearance observed in SHH at 4°C [$3.8 \pm 1.3 \mu\text{l}/(\text{min} \times \text{million cells})$]. However, a big difference was observed between active uptake clearance predicted from CHO cells [$1.9 \pm 0.3 \mu\text{l}/(\text{min} \times \text{million cells})$] and the measured active uptake clearance [$10.1 \pm 1.5 \mu\text{l}/(\text{min} \times \text{million cells})$]. The predicted OATP-mediated

uptake clearance in SHH [$1.9 \pm 0.3 \mu\text{l}/(\text{min} \times \text{million cells})$] only amounted to 14% of the observed total uptake clearance in SHH. However, this corresponds to the small (10%) but statistically insignificant change in vincristine uptake in the presence of the OATP transporter inhibitor rifamycin SV in SHH.

Identification of the benzbromarone-sensitive efflux transporter

Effect of 2 μM of MDR1 inhibitors elacridar, tariquidar and valspodar was assessed on the uptake of vincristine (Figure 5) in cryopreserved suspended rat and human hepatocytes to rule out the contribution of P-gp in vincristine efflux in suspended hepatocytes. No significant effect was observed of the MDR1 inhibitors on the uptake of vincristine whereas benzbromarone (100 μM) increased the uptake of vincristine in both species. To evaluate which MRP transporter could be involved in vincristine disposition in suspended hepatocytes, uptake of vincristine was assessed in MRP1, MRP2 and MRP3 inside-out membrane vesicles (Figure 6). No significant difference was observed in the uptake of vincristine in the presence of either ATP or AMP. To validate the vesicle assay for assessing vincristine efflux, we showed that in MDR1 vesicles vincristine uptake was significantly different in the presence of ATP (Figure 6) (14). Still, benzbromarone inhibited the ATP-dependent uptake of E17BDG and CDCF in MRP1, MRP2 and MRP3 vesicles. It is noteworthy that the absolute difference between CDCF uptake in control and MRP3 vesicles was low [$22 \text{ pmol}/(\text{min} \times \text{mg protein})$] as compared to CDCF uptake in MRP2 vesicles.

Discussion

Notwithstanding the fact that vincristine is one of the oldest anticancer drugs currently being used in clinical practice, some questions regarding vincristine pharmacokinetics remain unanswered (5). With respect to hepatic uptake, several studies during the early 90's investigated the uptake processes of vinca-alkaloids vincristine and vinblastine in human and rat hepatocytes. Based on these studies, the authors concluded that an energy-independent non-saturable passive diffusion process and an energy-dependent saturable active transport system may be involved in the uptake of vinca-alkaloids (34). More recently, several publications reported the interference of vincristine with OATP1B1 and OATP1B3-mediated uptake processes (30, 31). Additionally, in a thesis by T. Loo in 2011, SNPs in genes coding for SLCO1B1 and SLCO1B3 were positively correlated with the manifestation of vincristine-induced neurotoxicity (35). The present work was therefore aiming to elucidate the potential role of several isoforms of the OATP transporter family in the hepatocellular distribution of vincristine.

Experiments with suspended rat hepatocytes clearly showed that vincristine uptake was temperature-dependent, with a 7.6-fold lower uptake at 4°C (Figure 1). These data are in line with temperature-dependent uptake of vinblastine (2.6-fold lower uptake at 4°C) as shown by Zhou and coworkers (27). However, temperature-dependency not necessarily indicates that a transporter-mediated process is involved, since membrane fluidity may be reduced at 4°C (36, 37). To identify whether vincristine uptake was in fact mediated by one or more transporters, uptake experiments were performed in the presence of several known OATP inhibitors (Figure 1). Paclitaxel and docetaxel exhibited the most pronounced effect on vincristine uptake, confirming the strong interaction of taxanes with OATP transporters (30, 31). Inhibition of vincristine uptake in SRH by methotrexate is in line with research performed by Smeland et al.,

who suggested a competitive interaction between vincristine and methotrexate in SRH (29). However, digoxin and quinidine, both OATP1A4/*Slc21a5* inhibitors, were unable to significantly alter the vincristine uptake process (38). This indicates that vincristine is probably not a good substrate for OATP1A4. All other OATP inhibitors (atazanavir, bromosulphophthalein, cyclosporine A, glibenclamide, losartan, rifampicin and rifamycin SV) inhibited vincristine uptake to a similar extent (40% decrease). Even the well-known MRP inhibitor MK571 was able to reduce vincristine entry into SRH. This was not unexpected, since several research groups have reported that MK571 is a potent inhibitor of OATP transporters (31). Uptake experiments of vincristine in OATP1B1-, 1B3- and 2B1-transfected CHO cell lines resulted in a higher vincristine uptake as compared to wild-type CHO cells (Figure 3A). Additionally, uptake of vincristine in transfected CHO cells could be inhibited with a series of OATP transporter inhibitors (Figures 3B-D). OATP-mediated uptake of vincristine proved to be non-saturable with concentrations up to 300 μ M (data not shown). Uptake data of vincristine in OATP1B1- and OATP1B3-transfected CHO cells were converted for comparison with SHH data by using RAF factors which were determined previously by our group (33). Passive uptake data estimated from vincristine uptake in wild-type CHO cells [$4.1 \pm 0.5 \mu\text{l}/(\text{min} \times \text{million cells})$] corresponded well to passive uptake clearance observed in SHH at 4°C [$3.8 \pm 1.3 \mu\text{l}/(\text{min} \times \text{million cells})$] (Table 3). However, uptake measurements obtained at 4°C likely underestimate true passive uptake due to increased membrane rigidity at low temperature (36, 37). RAF-corrected total uptake clearance [$1.9 \pm 0.3 \mu\text{l}/(\text{min} \times \text{million cells})$] valued 15% of the observed total uptake clearance in SHH [$13.9 \pm 3.7 \mu\text{l}/(\text{min} \times \text{million cells})$]. This appears consistent with the fact that uptake of vincristine in SHH could not be inhibited below 90%, using an established OATP transporter inhibitor such as rifamycin SV (Figure 4B). It is still plausible that rifamycin SV simultaneously inhibited uptake as well as efflux transport (39). As a consequence, inhibition of vincristine

uptake would be counteracted by the inhibition of vincristine efflux transport, resulting in an insignificant net decrease of 10%. Also, involvement of another unidentified uptake transporter could explain the large observed difference between uptake at 37°C and 4°C which was not explained by the inhibition of OATP. In view of the relatively large size of vincristine, the involvement of OAT2 in hepatic uptake of vincristine can be considered less likely, although we cannot exclude this based on the presently available data. Still, rifamycin SV statistically significantly decreased vincristine uptake in one batch of SHH by 52.5%. It is also possible that this individual (Asian; male; 55 years old) carries a SNP in one of the OATP-coding genes, corresponding to a phenotype with increased vincristine uptake. On the other hand, the benzbromarone-sensitive efflux transporter may have been less active in this individual, thus improving conditions to observe OATP inhibition in the presence of rifamycin SV.

Apart from the observed uptake inhibition, increasing concentrations of MK571 and benzbromarone significantly increased the uptake of vincristine in SRH (Figures 2A-B). This contrasts to a previous study of Zhou and coworkers, where it was suggested that vincristine efflux in suspended hepatocytes was limited (27). Similar results were obtained in SHH in the presence of 100 μ M of benzbromarone (Figure 4C). Both MK571 and benzbromarone are established MRP transporter inhibitors, implying the role of an MRP transporter in the hepatic disposition of vincristine (40). Cis-stimulation of the OATP-mediated uptake by benzbromarone was ruled out, since it did not increase the uptake of vincristine in the OATP-transfected-CHO cells (41). Since vincristine is a well-known MDR1 substrate, we needed to show that benzbromarone and MK571 did not inhibit MDR1 in suspended hepatocytes. This was indeed ruled out since selective MDR1 inhibitors elacridar, tariquidar and valspodar did not increase the accumulation of vincristine in suspended rat and human hepatocytes (Figure 5). This is in line

with the internalization of MDR1 in suspended hepatocytes as reported by Bow and coworkers (42). Involvement of BCRP was also excluded since it was reported that BCRP did not confer resistance to vincristine and internalization of MDR1 would also imply the internalization of other canalicular membranes. Among the MRP transporters, it was reported in literature that MRP4, MRP5 and MRP6 expression in transfected cell lines did not induce resistance to vincristine toxicity (43-45). On the other hand, it is well known that vincristine is a substrate of MRP1. However, hepatic MRP1 expression levels in adult hepatocytes are generally considered low or non-detectable (46). This reduces the likelihood for MRP1 to have a considerable impact on hepatic drug disposition. Presence of MRP2 had also shown to confer resistance to vincristine toxicity (16, 47-49). However, since we were unable to increase vincristine accumulation in the presence of MDR1-selective inhibitors, we hypothesized that MRP2 would likewise not be present or active on the membrane of suspended hepatocytes (42). Several reports claim that expression of MRP3 could be linked to vincristine resistance; however literature reports on MRP3-mediated vincristine transport are unclear (50-53). Taken together, it seems that MRP3 is the only known transporter present in suspended hepatocytes likely to mediate vincristine efflux. To verify which transporter mediated vincristine efflux, vincristine uptake was assessed in membrane vesicles containing MRP1, MRP2, MRP3. However, we were not able to detect the transport of vincristine by MRP1, MRP2 or MRP3 (Figure 6). To ensure that the vesicle assay is a suitable system to measure vincristine transport, we showed that we were able to measure the ATP-dependent transport of vincristine by MDR1. Still, the hydrophobic nature of vincristine could hinder the accurate measurement of vincristine transport in MRP1, MRP2 and MRP3 containing membrane vesicles. It is known that it is challenging to assess efflux transport of hydrophobic compounds in inside-out membrane vesicles (54). Due to this drawback of the *in vitro* system, we do not conclude that vincristine is not transported by MRP1, MRP2 or MRP3. It

may also be possible that the expression levels of MRP3 were too low in the currently used membrane vesicles to measure the transport of vincristine. Indeed, CDCF transport in control and MRP3 containing vesicles did not differ greatly but the uptake could still be inhibited by benzbromarone (Figure 7). In a thesis by Loo in 2011, a wide range of ABC transporters were significantly correlated with vincristine neurotoxicity (ABCA4, ABCB5, ABCG1, ABCC4, ABCA1, ABCC1/6, ABCB1, ABCC8, ABCC3, ABCC10, ABCC2) (35). Instead of toxicity studies, actual transport of vincristine should be evaluated in transfected cell lines or membrane vesicles containing other transporters to identify which transporters are involved. Alternatively, inhibition studies with selective MRP inhibitors could help to identify this elusive efflux transporter. A transporter of the MRP family likely corresponds to the unidentified efflux transporter since benzbromarone and MK571 are notorious MRP inhibitors. However, MRP transporters require ATP for their activity and Watanabe and coworkers reported no change in the uptake of vincristine in SRH upon depletion of ATP (55). Thus, an ATP-independent benzbromarone-sensitive efflux transporter, not related to the MRP family, may also be responsible for vincristine efflux in SRH (e.g. MATE1, OST α/β). Further research is therefore warranted to elucidate the identity of this important transporter for hepatocellular vincristine disposition.

Conclusion

In conclusion, OATP transporters are involved in the disposition of vincristine in suspended rat and human hepatocytes. However, efflux transport, potentially by the sinusoidal efflux transporter MRP3, overshadows the effect of OATP-mediated transport. The exact role of uptake and efflux transporters should be further investigated to enable mechanistic modeling of vincristine disposition. The present and future findings on vincristine disposition pathways could help researchers to explain the large inter-individual variability in vincristine exposure and improve patient-specific dose selection.

Acknowledgements

The authors would like to thank Bioreclamation IVT[®] for kindly providing human hepatocytes. Johan Nicolai received a PhD scholarship from the Agency for Innovation by Science and Technology [Agentschap voor innovatie door wetenschap en technologie (IWT), Flanders, Belgium], project number 111193. This study was partially supported by FWO grant G.0662.09N and by internal funds of Drug Delivery and Disposition, KU Leuven Department of Pharmaceutical and Pharmacological Sciences.

References

1. Johnson IS, Armstrong JG, Gorman M, Burnett JP, Jr. The Vinca Alkaloids: A New Class of Oncolytic Agents. *Cancer Res.* 1963;23:1390-427.
2. Estlin EJ, Ronghe M, Burke GA, Yule SM. The clinical and cellular pharmacology of vincristine, corticosteroids, L-asparaginase, anthracyclines and cyclophosphamide in relation to childhood acute lymphoblastic leukaemia. *Br J Haematol.* 2000;110(4):780-90.
3. van Hasselt JG, van Eijkelenburg NK, Beijnen JH, Schellens JH, Huitema AD. Design of a drug-drug interaction study of vincristine with azole antifungals in pediatric cancer patients using clinical trial simulation. *Pediatr Blood Cancer.* 2014;61(12):2223-9.
4. [Available from: <https://www.cancer.gov/about-cancer/treatment/drugs/vincristinesulfate>.
5. Gidding CE, Kellie SJ, Kamps WA, de Graaf SS. Vincristine revisited. *Crit Rev Oncol Hematol.* 1999;29(3):267-87.
6. Gillet JP, Gottesman MM. Mechanisms of multidrug resistance in cancer. *Methods Mol Biol.* 2010;596:47-76.
7. Van den Berg HW, Desai ZR, Wilson R, Kennedy G, Bridges JM, Shanks RG. The pharmacokinetics of vincristine in man: reduced drug clearance associated with raised serum alkaline phosphatase and dose-limited elimination. *Cancer Chemother Pharmacol.* 1982;8(2):215-9.
8. Jackson DV, Jr., Castle MC, Bender RA. Biliary excretion of vincristine. *Clin Pharmacol Ther.* 1978;24(1):101-7.
9. Egbelakin A, Ferguson MJ, MacGill EA, Lehmann AS, Topletz AR, Quinney SK, et al. Increased risk of vincristine neurotoxicity associated with low CYP3A5 expression genotype in children with acute lymphoblastic leukemia. *Pediatr Blood Cancer.* 2011;56(3):361-7.

10. van Schie RM, Bruggemann RJ, Hoogerbrugge PM, te Loo DM. Effect of azole antifungal therapy on vincristine toxicity in childhood acute lymphoblastic leukaemia. *J Antimicrob Chemother.* 2011;66(8):1853-6.
11. Dennison JB, Kulanthaivel P, Barbusch RJ, Renbarger JL, Ehlhardt WJ, Hall SD. Selective metabolism of vincristine in vitro by CYP3A5. *Drug Metab Dispos.* 2006;34(8):1317-27.
12. Dennison JB, Jones DR, Renbarger JL, Hall SD. Effect of CYP3A5 expression on vincristine metabolism with human liver microsomes. *J Pharmacol Exp Ther.* 2007;321(2):553-63.
13. Dennison JB, Mohutsky MA, Barbusch RJ, Wrighton SA, Hall SD. Apparent high CYP3A5 expression is required for significant metabolism of vincristine by human cryopreserved hepatocytes. *J Pharmacol Exp Ther.* 2008;327(1):248-57.
14. Hooiveld GJ, Heegsma J, van Montfoort JE, Jansen PL, Meijer DK, Muller M. Stereoselective transport of hydrophilic quaternary drugs by human MDR1 and rat Mdr1b P-glycoproteins. *Br J Pharmacol.* 2002;135(7):1685-94.
15. Loe DW, Deeley RG, Cole SP. Characterization of vincristine transport by the M(r) 190,000 multidrug resistance protein (MRP): evidence for cotransport with reduced glutathione. *Cancer Res.* 1998;58(22):5130-6.
16. Kawabe T, Chen ZS, Wada M, Uchiumi T, Ono M, Akiyama S, et al. Enhanced transport of anticancer agents and leukotriene C4 by the human canalicular multispecific organic anion transporter (cMOAT/MRP2). *FEBS Lett.* 1999;456(2):327-31.
17. Kool M, van der Linden M, de Haas M, Scheffer GL, de Vree JM, Smith AJ, et al. MRP3, an organic anion transporter able to transport anti-cancer drugs. *Proc Natl Acad Sci U S A.* 1999;96(12):6914-9.

18. Hopper-Borge E, Chen ZS, Shchaveleva I, Belinsky MG, Kruh GD. Analysis of the drug resistance profile of multidrug resistance protein 7 (ABCC10): resistance to docetaxel. *Cancer Res.* 2004;64(14):4927-30.
19. Minami K, Kamijo Y, Nishizawa Y, Tabata S, Horikuchi F, Yamamoto M, et al. Expression of ABCB6 is related to resistance to 5-FU, SN-38 and vincristine. *Anticancer Res.* 2014;34(9):4767-73.
20. Drake KJ, Singhal J, Yadav S, Nadkar A, Pungaliya C, Singhal SS, et al. RALBP1/RLIP76 mediates multidrug resistance. *Int J Oncol.* 2007;30(1):139-44.
21. Mandery K, Glaeser H, Fromm MF. Interaction of innovative small molecule drugs used for cancer therapy with drug transporters. *Br J Pharmacol.* 2012;165(2):345-62.
22. Buxhofer-Ausch V, Secky L, Wlcek K, Svoboda M, Kounnis V, Briasoulis E, et al. Tumor-specific expression of organic anion-transporting polypeptides: transporters as novel targets for cancer therapy. *J Drug Deliv.* 2013;2013:863539.
23. Liu T, Li Q. Organic anion-transporting polypeptides: a novel approach for cancer therapy. *J Drug Target.* 2014;22(1):14-22.
24. Shnitsar V, Eckardt R, Gupta S, Grottke J, Muller GA, Koepsell H, et al. Expression of human organic cation transporter 3 in kidney carcinoma cell lines increases chemosensitivity to melphalan, irinotecan, and vincristine. *Cancer Res.* 2009;69(4):1494-501.
25. Bleyer WA, Frisby SA, Oliverio VT. Uptake and binding of vincristine by murine leukemia cells. *Biochem Pharmacol.* 1975;24(5):633-9.
26. Ferguson PJ, Cass CE. Differential cellular retention of vincristine and vinblastine by cultured human promyelocytic leukemia HL-60/Cl cells: the basis of differential toxicity. *Cancer Res.* 1985;45(11 Pt 1):5480-8.

27. Zhou XJ, Martin M, Placidi M, Cano JP, Rahmani R. In vivo and in vitro pharmacokinetics and metabolism of vincaalkaloids in rat. II. Vinblastine and vincristine. *Eur J Drug Metab Pharmacokinet.* 1990;15(4):323-32.
28. Zhou XJ, Rahmani R. Preclinical and clinical pharmacology of vinca alkaloids. *Drugs.* 1992;44 Suppl 4:1-16; discussion 66-9.
29. Smeland E, Bremnes RM, Bessesen A, Jaeger R, Aarbakke J. Interactions of vinblastine and vincristine with methotrexate transport in isolated rat hepatocytes. *Cancer Chemother Pharmacol.* 1993;32(3):209-14.
30. Yamaguchi H, Kobayashi M, Okada M, Takeuchi T, Unno M, Abe T, et al. Rapid screening of antineoplastic candidates for the human organic anion transporter OATP1B3 substrates using fluorescent probes. *Cancer Lett.* 2008;260(1-2):163-9.
31. Karlgren M, Ahlin G, Bergstrom CA, Svensson R, Palm J, Artursson P. In vitro and in silico strategies to identify OATP1B1 inhibitors and predict clinical drug-drug interactions. *Pharm Res.* 2012;29(2):411-26.
32. Nicolai J, De Bruyn T, Van Veldhoven PP, Keemink J, Augustijns P, Annaert P. Verapamil hepatic clearance in four preclinical rat models: towards activity-based scaling. *Biopharm Drug Dispos.* 2015;36(7):462-80.
33. De Bruyn T, Stieger B, Augustijns PF, Annaert PP. Clearance Prediction of HIV Protease Inhibitors in Man: Role of Hepatic Uptake. *J Pharm Sci.* 2016;105(2):854-63.
34. Zhou XJ, Placidi M, Rahmani R. Uptake and metabolism of vinca alkaloids by freshly isolated human hepatocytes in suspension. *Anticancer Res.* 1994;14(3A):1017-22.
35. Loo T. The pharmacogenomics of vincristine-induced neurotoxicity in paediatric cancer patients with Wilms tumor and rhabdomyosarcoma. Vancouver: University of British Columbia; 2011.

36. Poirier A, Lave T, Portmann R, Brun ME, Senner F, Kansy M, et al. Design, data analysis, and simulation of in vitro drug transport kinetic experiments using a mechanistic in vitro model. *Drug Metab Dispos.* 2008;36(12):2434-44.
37. Sugano K, Kansy M, Artursson P, Avdeef A, Bendels S, Di L, et al. Coexistence of passive and carrier-mediated processes in drug transport. *Nat Rev Drug Discov.* 2010;9(8):597-614.
38. Shitara Y, Sugiyama D, Kusuhashi H, Kato Y, Abe T, Meier PJ, et al. Comparative inhibitory effects of different compounds on rat oatpl (slc21a1)- and Oatp2 (Slc21a5)-mediated transport. *Pharm Res.* 2002;19(2):147-53.
39. Kimoto E, Li R, Scialis RJ, Lai Y, Varma MV. Hepatic Disposition of Gemfibrozil and Its Major Metabolite Gemfibrozil 1-O-beta-Glucuronide. *Mol Pharm.* 2015;12(11):3943-52.
40. Bodo A, Bakos E, Szeri F, Varadi A, Sarkadi B. The role of multidrug transporters in drug availability, metabolism and toxicity. *Toxicol Lett.* 2003;140-141:133-43.
41. Gui C, Miao Y, Thompson L, Wahlgren B, Mock M, Stieger B, et al. Effect of pregnane X receptor ligands on transport mediated by human OATP1B1 and OATP1B3. *Eur J Pharmacol.* 2008;584(1):57-65.
42. Bow DA, Perry JL, Miller DS, Pritchard JB, Brouwer KL. Localization of P-gp (Abcb1) and Mrp2 (Abcc2) in freshly isolated rat hepatocytes. *Drug Metab Dispos.* 2008;36(1):198-202.
43. Belinsky MG, Chen ZS, Shchaveleva I, Zeng H, Kruh GD. Characterization of the drug resistance and transport properties of multidrug resistance protein 6 (MRP6, ABCC6). *Cancer Res.* 2002;62(21):6172-7.
44. Pratt S, Shepard RL, Kandasamy RA, Johnston PA, Perry W, 3rd, Dantzig AH. The multidrug resistance protein 5 (ABCC5) confers resistance to 5-fluorouracil and transports its monophosphorylated metabolites. *Mol Cancer Ther.* 2005;4(5):855-63.

45. Tian Q, Zhang J, Chan SY, Tan TM, Duan W, Huang M, et al. Topotecan is a substrate for multidrug resistance associated protein 4. *Curr Drug Metab*. 2006;7(1):105-18.
46. He SM, Li R, Kanwar JR, Zhou SF. Structural and functional properties of human multidrug resistance protein 1 (MRP1/ABCC1). *Curr Med Chem*. 2011;18(3):439-81.
47. Koike K, Kawabe T, Tanaka T, Toh S, Uchiumi T, Wada M, et al. A canalicular multispecific organic anion transporter (cMOAT) antisense cDNA enhances drug sensitivity in human hepatic cancer cells. *Cancer Res*. 1997;57(24):5475-9.
48. Cui Y, Konig J, Buchholz JK, Spring H, Leier I, Keppler D. Drug resistance and ATP-dependent conjugate transport mediated by the apical multidrug resistance protein, MRP2, permanently expressed in human and canine cells. *Mol Pharmacol*. 1999;55(5):929-37.
49. van Zanden JJ, de Mul A, Wortelboer HM, Usta M, van Bladeren PJ, Rietjens IM, et al. Reversal of in vitro cellular MRP1 and MRP2 mediated vincristine resistance by the flavonoid myricetin. *Biochem Pharmacol*. 2005;69(11):1657-65.
50. Zeng H, Bain LJ, Belinsky MG, Kruh GD. Expression of multidrug resistance protein-3 (multispecific organic anion transporter-D) in human embryonic kidney 293 cells confers resistance to anticancer agents. *Cancer Res*. 1999;59(23):5964-7.
51. Zelcer N, Saeki T, Reid G, Beijnen JH, Borst P. Characterization of drug transport by the human multidrug resistance protein 3 (ABCC3). *J Biol Chem*. 2001;276(49):46400-7.
52. Huang R, Murry DJ, Kolwankar D, Hall SD, Foster DR. Vincristine transcriptional regulation of efflux drug transporters in carcinoma cell lines. *Biochem Pharmacol*. 2006;71(12):1695-704.
53. Grant CE, Gao M, DeGorter MK, Cole SP, Deeley RG. Structural determinants of substrate specificity differences between human multidrug resistance protein (MRP) 1 (ABCC1) and MRP3 (ABCC3). *Drug Metab Dispos*. 2008;36(12):2571-81.

54. International Transporter C, Giacomini KM, Huang SM, Tweedie DJ, Benet LZ, Brouwer KL, et al. Membrane transporters in drug development. *Nat Rev Drug Discov.* 2010;9(3):215-36.
55. Watanabe T, Miyauchi S, Sawada Y, Iga T, Hanano M, Inaba M, et al. Kinetic analysis of hepatobiliary transport of vincristine in perfused rat liver. Possible roles of P-glycoprotein in biliary excretion of vincristine. *J Hepatol.* 1992;16(1-2):77-88.

Tables

Table 1. Demographic and medical information on human hepatocyte donors used in the current study and used in the article by De Bruyn and coworkers to calculate the RAF factors for *OATP1B1* and *OATP1B3* (33).

Batch	Sex	Age	Race	Cause of death	Medical history
YUA	M	40	Caucasian	Stroke	Alcohol use, tobacco use, medication for hypertension
QWG	F	58	Caucasian	CVA	NA.
HRU	M	55	Asian	Intracranial bleed	NA.
JCM	F	77	Caucasian	Intracranial bleed	Alcohol (2-3 drinks per month)
MNO	M	80	Caucasian	CVA	Tobacco use
KCM	F	40	Black	Intracranial bleed	Alcohol use, tobacco, potentially marijuana, medication for hypertension, diabetes and cholesterol
GUY	M	39	Caucasian	Intracranial bleed	Cocaine use, alcohol use
FDX*	10M/10F	52	17C, 2B, 1H	***	***
ZKO**	25M/25F	54	42C, 5B, 3H	***	***
RAF-Pool (33)	2M/3F	43	Caucasian	#	#

Age in years, average age depicted for donor pools, * 20-donor pool, **50-donor pool, *** information can be requested from Bioreclamation IVT, RAF-Pool refers to the batch of pooled human hepatocytes used by De Bruyn and coworkers to calculate the RAF factors for *OATP1B1* and *OATP1B3* (33), # information can be requested from CellzDirectTM for batches Hu4050, Hu8067, Hu4140, Hu4128 and Hu8008.

Table 2. Relative activity factors (RAF) applied to calculate vincristine uptake clearance in SHH from vincristine uptake in OATP1B1- and OATP1B3-transfected CHO-cells.

RAF-factor	Estrone-3-sulfate	CGamF
RAF _{OATP1B1}	0.70	N.A.
RAF _{OATP1B3}	N.A.	0.11

RAF factors for these cell-lines were determined previously within our research group (33) by comparison with a pool of suspended human hepatocytes.

Table 3. Vincristine uptake clearance [$\mu\text{L}/(\text{min} \times \text{million cells})$] in CHO cells, corrected with RAF factors for OATP1B1 and OATP1B3 activities (Table 2), compared to average vincristine uptake clearance values in SHH.

Cell line	Cl _{CHO}	Cl _{SHH,estimated}	Condition	Cl _{SHH,observed}
wild-type	2.1 \pm 0.2	4.1 \pm 0.5	4°C	3.8 \pm 1.3
OATP1B1	1.9 \pm 0.4	1.3 \pm 0.3	/	/
OATP1B3	5.7 \pm 0.5	0.6 \pm 0.1	/	/
Total _{OATP}	/	1.9 \pm 0.3	37°C-4°C	10.1 \pm 1.5
Total	/	6.0 \pm 0.6	37°C	13.9 \pm 3.7

Cl_{CHO}: vincristine uptake clearance in CHO cells, Cl_{SHH,estimated}: vincristine uptake clearance from CHO-cells which has been recalculated with RAF factors, Cl_{SHH,observed}: vincristine uptake clearance observed in SHH experiments. Values represent means \pm SD.

Legend to Figures

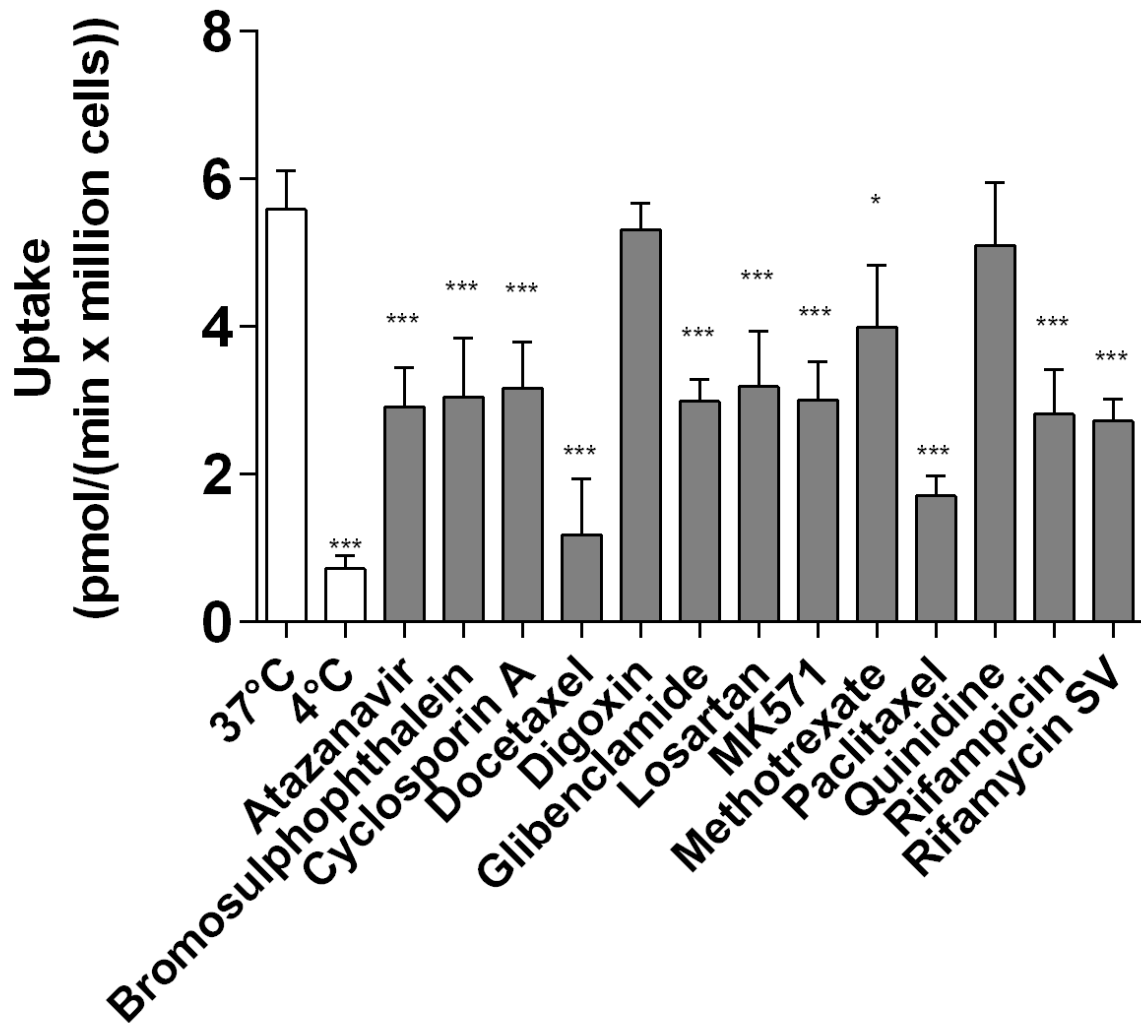


Figure 1. Effect of temperature and OATP inhibitors (10 μ M) on the uptake of vincristine (0.5 μ M) in SRH. Every inhibitor except for digoxin and quinidine significantly inhibited vincristine uptake. Bars represent means \pm SD of triplicate incubations in two preparations of SRH. Conditions were compared to uptake at 37°C in SRH. (* $p < 0.05$; *** $p < 0.001$)

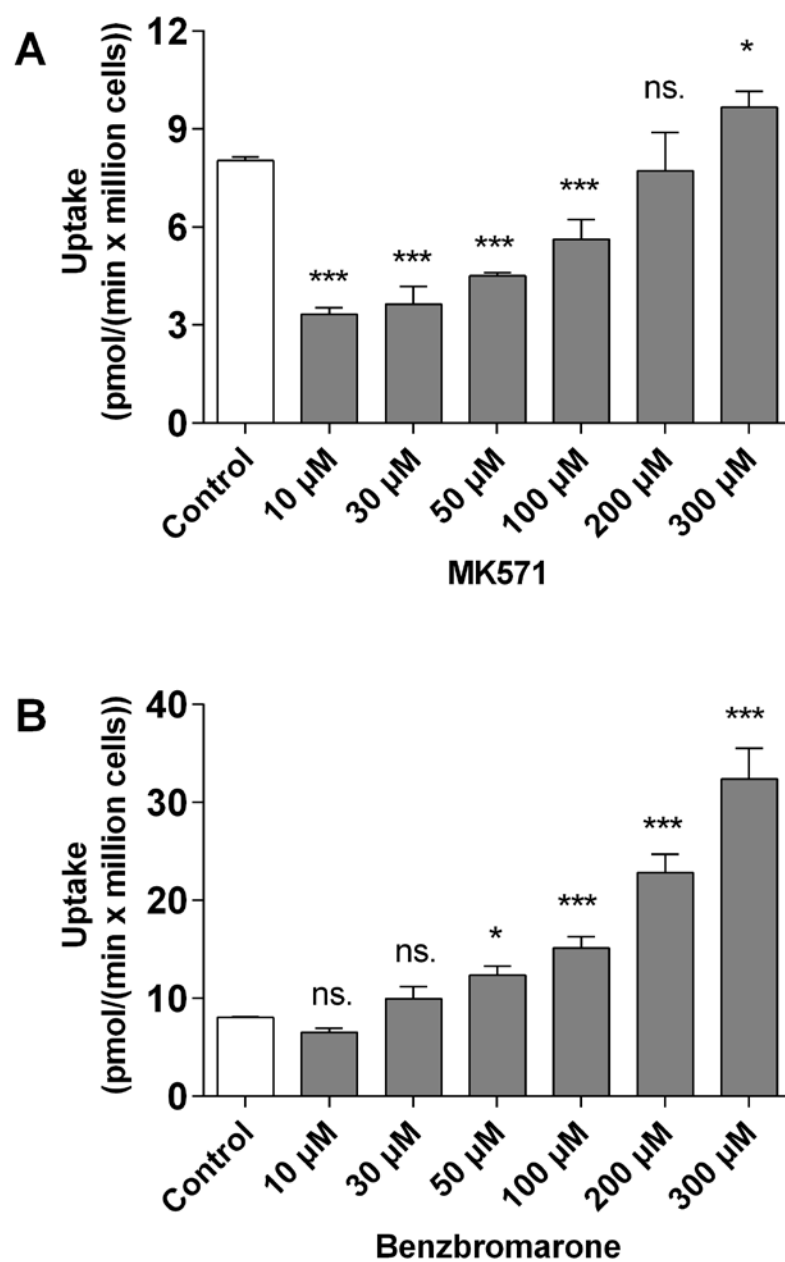


Figure 2. Effect of increasing concentrations of MRP inhibitors MK571 (A) and benzbromarone (B) on the uptake of vincristine (0.5 μ M) in SRH as compared to the control condition (white bar). Bars represent means \pm SD of triplicate incubations in one batch of SRH. (ns. not significant; * $p < 0.05$; *** $p < 0.001$)

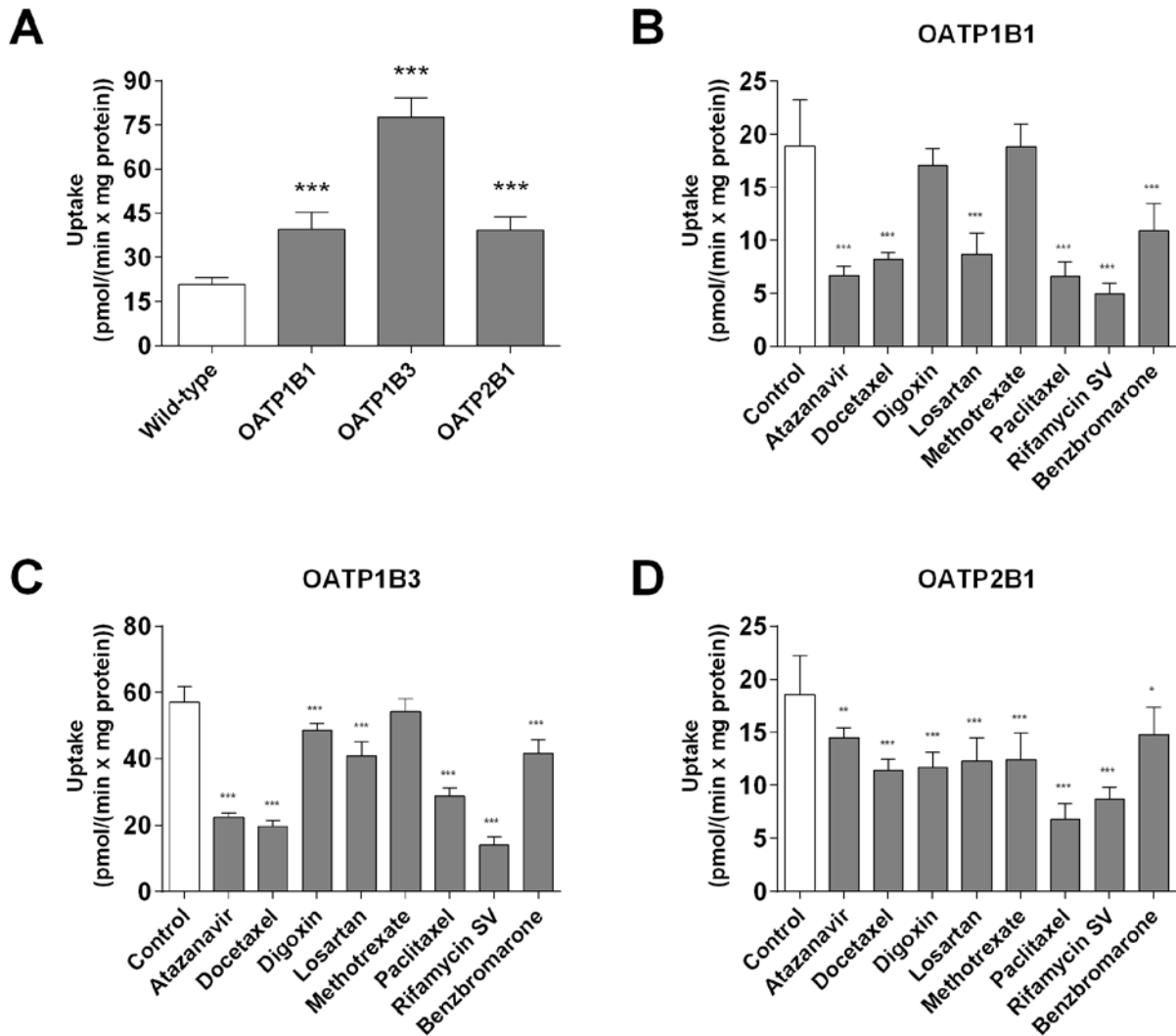


Figure 3. (A) Comparison of vincristine (10 μ M) uptake in wild-type and OATP1B1-, 1B3- and 2B1-transfected CHO-cells. Uptake of vincristine was significantly higher in all transfected CHO-cells as compared to the uptake in wild-type cells. (B-D) Effect of different OATP inhibitors (10 μ M) on the net uptake (wild-type subtracted uptake) of vincristine in OATP1B1-, OATP1B3- and OATP2B1-transfected CHO-cells. Bars represent means \pm SD of triplicate incubations in two preparations of CHO-cells. (* $p < 0.05$; ** $p < 0.01$; *** $p < 0.001$)

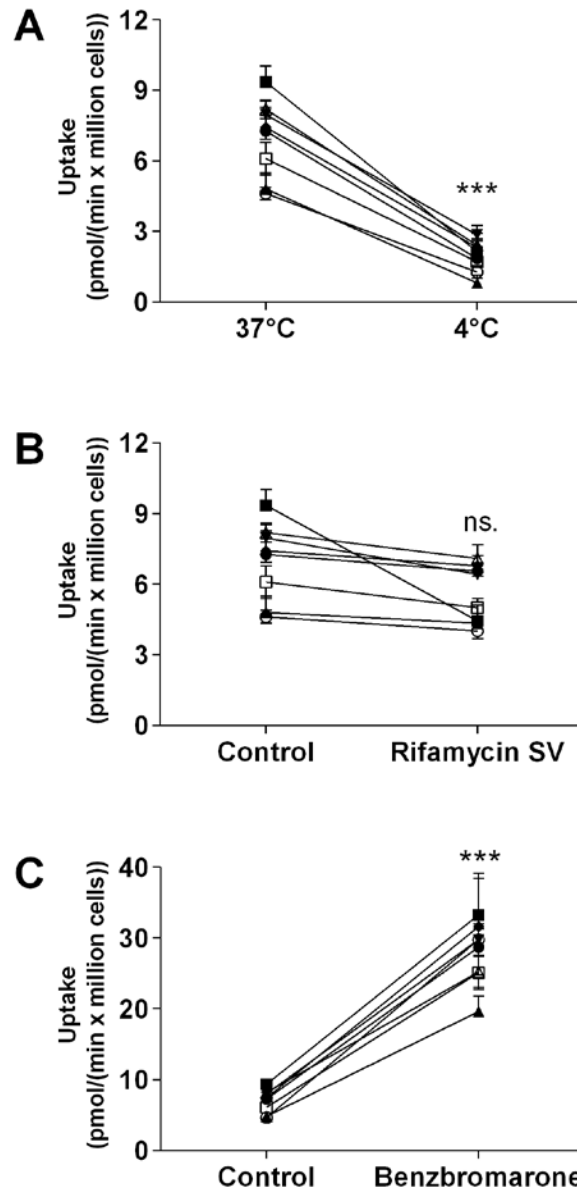


Figure 4. Effect of temperature (A), rifamycin SV (B) and benzbromarone (C) on the uptake of vincristine (0.5 μM) in SHH. Points represent the means of triplicate incubations in multiple batches ($n = 8$) of SHH. (ns. not significant; *** $p < 0.001$) Paired Student's t -tests were used to compare groups in all conditions (data were normally distributed). Uptake of vincristine only differed statistically significantly in one batch of SHH (HRU; $p = 0.0057$; 6B). Each symbol represents a different batch of SHH.

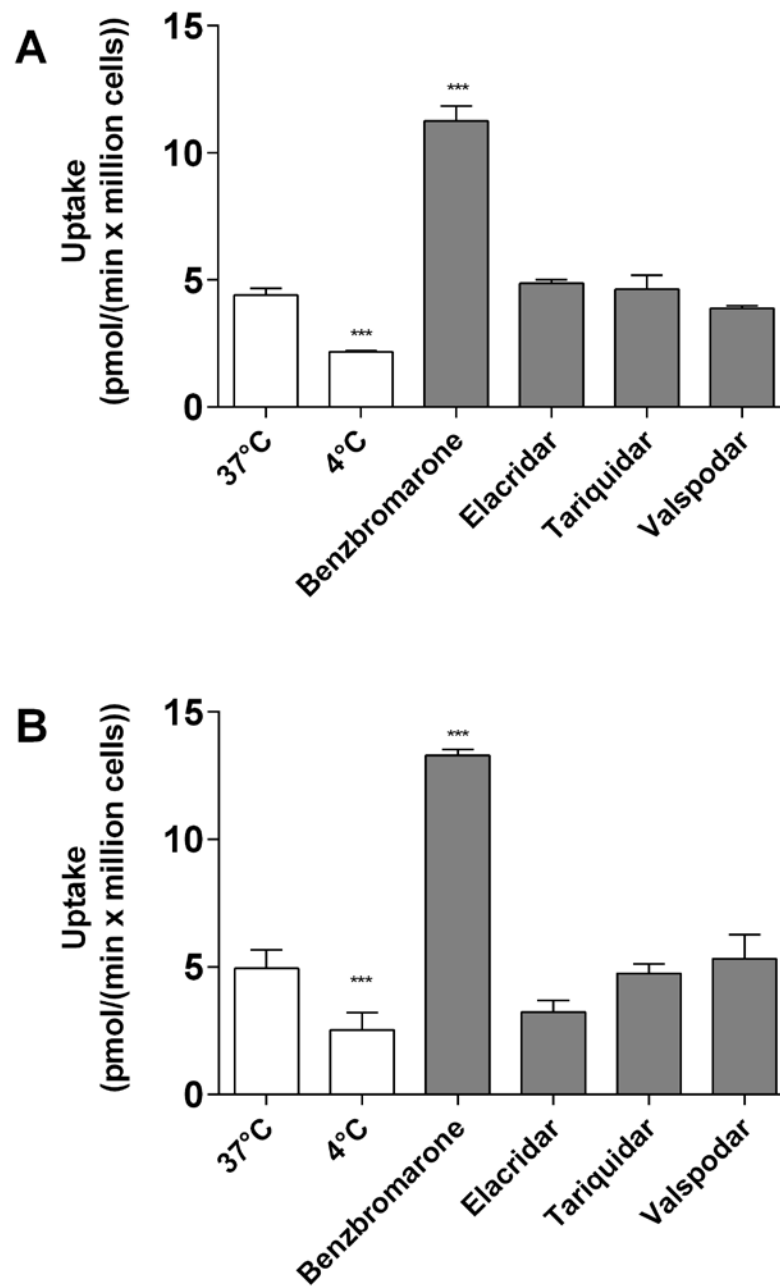


Figure 5. Effect of temperature, benzbromarone (100 μM) and selective P-gp inhibitors elacridar, tariquidar and valsopodar (2 μM) on the uptake of vincristine (0.5 μM) in (A) cryopreserved rat hepatocytes and (B) cryopreserved human hepatocytes. Bars represent means \pm SD of triplicate incubations in single batches of hepatocytes. (*** $p < 0.001$)

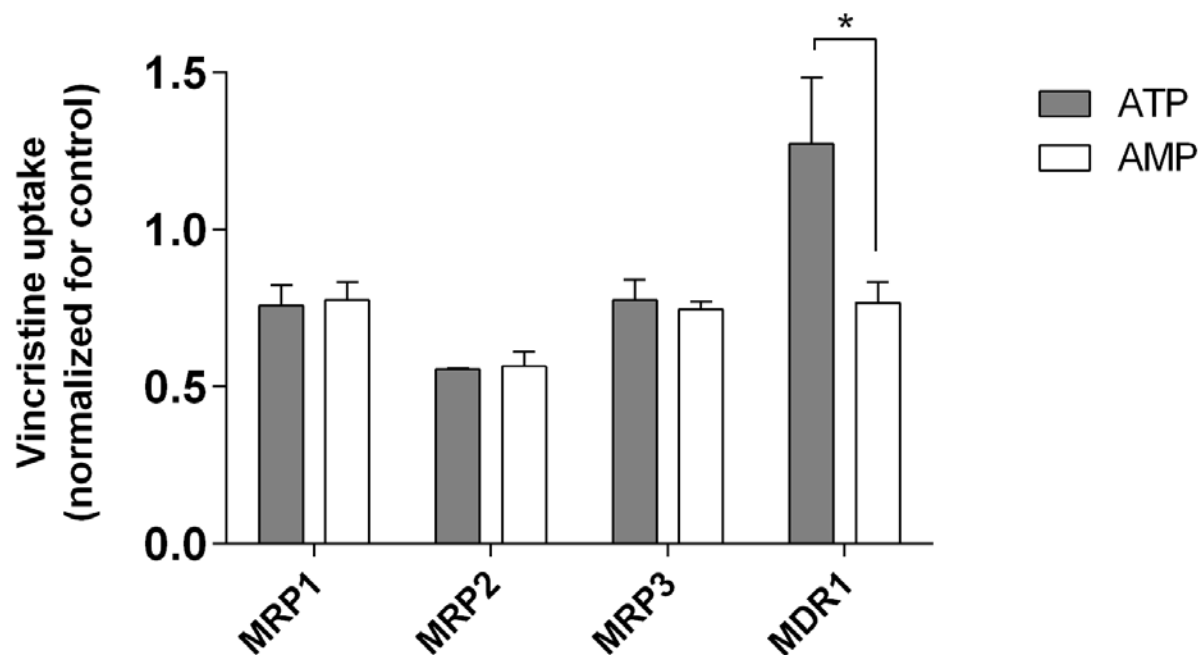


Figure 6. Uptake of vincristine (200 nM) in inside-out membrane vesicles containing MRP1, MRP2, MRP3 or MDR1, normalized for uptake in control vesicles in presence of either ATP or AMP. Bars represent means \pm SD of triplicate incubations in single batches of inside-out membrane vesicles. (* $p < 0.05$)

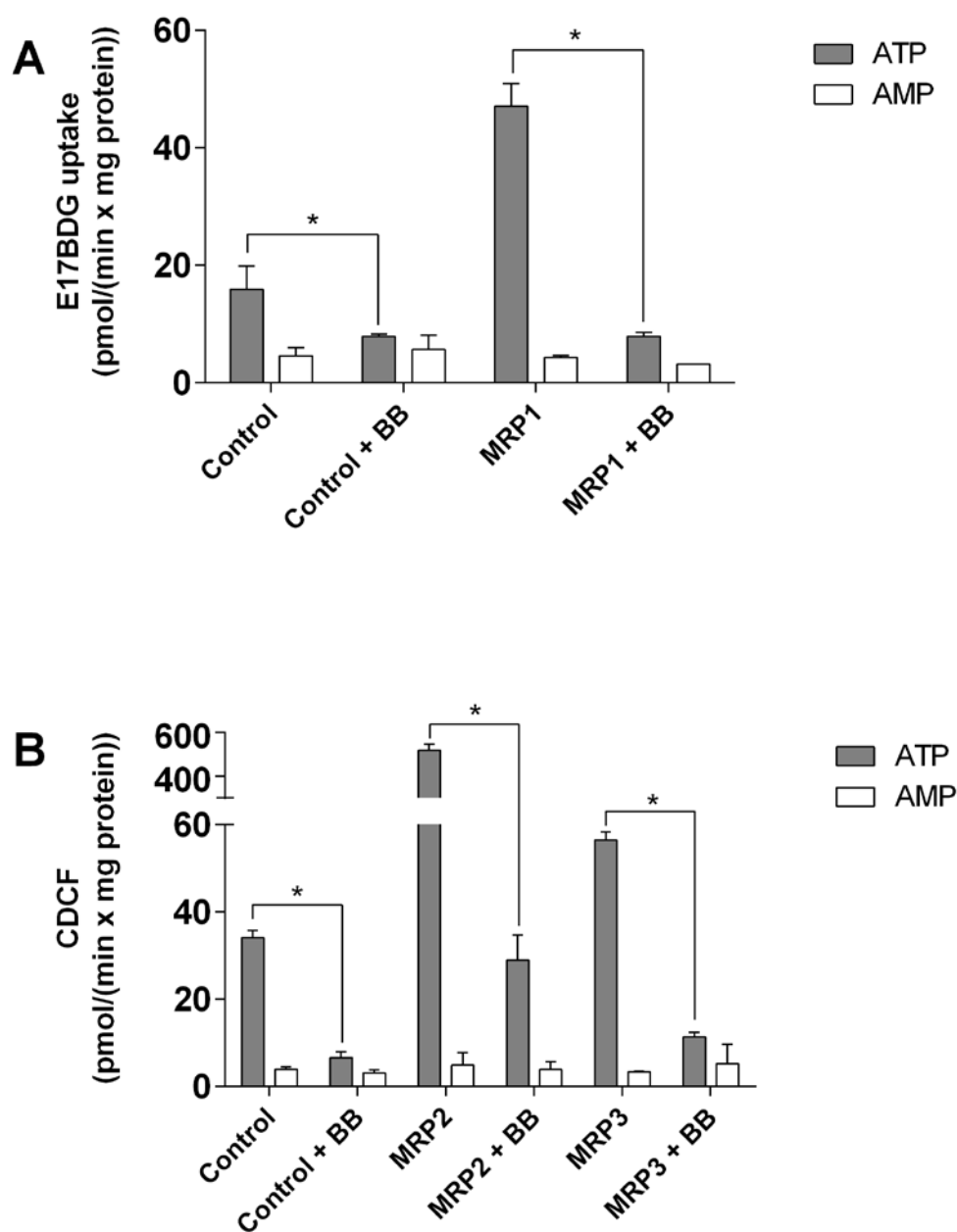


Figure 7. (A) Uptake of E17BDG ($10 \mu\text{M}$) in control and MRP1 containing inside-out membrane vesicles. (B) Uptake of CDCF ($10 \mu\text{M}$) in control, MRP2 and MRP3 containing inside-out membrane vesicles in presence of either ATP or AMP with or without benzbromarone ($100 \mu\text{M}$). Bars represent means \pm SD of triplicate incubations in single batches of inside-out membrane vesicles. (* $p < 0.05$).